Organometallics **2007,** *26,* 272−280

Inhibition of the *fac*-$(RCO_2)Re^I(CO_3)$(bis-azine) Photodecarboxylation of the Carboxylate Ligand, RCO_2^-, When R Is a Strongly Electron Donating Group: Thermal and Photochemical Properties of Complexes Where R = Ferrocene, 4-(Dimethylamino)benzyl

M. P. Juliarena,[†] G. T. Ruiz,[‡] E. Wolcan,[†] R. O. Lezna,[†] M. R. Feliz,*[,†] G. Ferraudi,*[,‡] and J. Guerrero[§]

INIFTA, Universidad Nacional de La Plata, C. C. 16, Suc. 4, 1900 La Plata, Argentina, Radiation Laboratory, University of Notre Dame, Notre Dame, Indiana 46556-0579, and Department of Applied Chemistry, Facultad de Química y Biología, Universidad de Santiago, Casilla 40, Correo 33, Santiago, Chile

Received May 30, 2006

The photophysical and phtochemical properties of *fac*-$(RCO_2)Re^I(CO)_3L$ (R = ferrocene, L = phen, 2,2′-bpy; R = 4-(dimethylamino)benzyl (4-DMAB), L = phen) were investigated with continuous and flash photolyses. Their properties were compared with those of *fac*-$(CH_3CO_2)Re^I(CO)_3L$ (L = phen, 2,2′-bpy) complexes. On a femtosecond to 10 ps time scale, the transient spectra of the singlet Re(I) to L charge-transfer excited states, $^1MLCT_{Re\rightarrow L}$, of *fac*-$(RCO_2)Re^I(CO)_3L$ (R = ferrocene, 4-DMAB) transform into the spectra of two triplet excited states, the $^3MLCT_{Re\rightarrow L}$ excited state and a Re(I) to RCO_2^- charge-transfer excited state, $^3MLCT_{Re\rightarrow RCO_2}$. The $^3MLCT_{Re\rightarrow RCO_2}$ and $^3MLCT_{Re\rightarrow L}$ excited states have lifetimes that span 10^2 ns to several microseconds. The photodecarboxylation of *fac*-$(RCO_2)Re^I(CO)_3L$, initiated in ligand-to-ligand charge-transfer excited states, $^3LLCT_{Re\rightarrow L}$, is markedly affected by the positions of the $^3MLCT_{Re\rightarrow RCO_2}$ and $^3MLCT_{Re\rightarrow L}$ excited states. In addition, the low energy of $^3LLCT_{RCO_2\rightarrow L}$ in the *fac*-$(RCO_2)Re^I(CO)_3L$ (L = phen, 2,2′-bpy) complexes, relative to those of *fac*-$(CH_3CO_2)Re^I(CO)_3L$ (L = phen, 2,2′-bpy) decreases the efficiency of the photodecarboxylation reaction.

Introduction

Photoprocesses involving the spectator ligand, X, of *fac*-$XRe^I(CO)_3Y$ (Y = bis(monoazine), bisazine) have been observed in a number of cases.[1−9] However, they are rare in comparison to the photogeneration of the luminescent metal-to-ligand charge transfer, $MLCT_{Re\rightarrow Y}$, and/or intraligand, IL, excited states. Metal-to-ligand charge transfer excited states involving the spectator ligand X, $^3MLCT_{Re\rightarrow 4-nitrobenzylCO_2}$, are formed in the photolysis of *fac*-(4-nitrobenzylCO_2)$Re^I(CO)_3$(2,2′-bpy).[6] A multistep mechanism leads to the indirect formation of this excited state (eqs 1−3).

$$fac\text{-}(4\text{−nitrobenzyl}CO_2)Re^I(CO)_3(2,2'\text{-bpy}) \xrightarrow{h\nu} {}^3MLCT_{Re\rightarrow 2,2'-bpy} \quad (1)$$

$$^3MLCT_{Re\rightarrow 2,2'-bpy} \rightleftarrows \text{intermediate} \quad (2)$$

$$\text{intermediate} \rightarrow {}^3MLCT_{Re\rightarrow 4-nitrobenzylCO_2} \quad (3)$$

The $^3MLCT_{Re\rightarrow 2,2'-bpy}$ excited state, produced in less than 20 ps (eq 1), is equilibrated with an intermediate species (eq 2). An irreversible process converts this intermediate into the long-lived and luminescent $^3MLCT_{Re\rightarrow 4-O_2NC_6H_4CO_2}$ excited state (eq 3). The absorption spectrum of the $^3MLCT_{Re\rightarrow 4-O_2NC_6H_4CO_2}$ excited-state showed the spectroscopic features of the 4-nitrobenzyl$^{\bullet -}$ chromophore.

In contrast to the photobehavior of *fac*-(4-nitrobenzylCO_2)-$Re^I(CO)_3$(2,2′-bpy), photolysis of the carboxylate complexes *fac*-$(RCO_2)Re^I(CO)_3$(2,2′-bpy) (R = methyl, 1-pyrenyl, 9-anthranyl, 2-naphthyl) at wavelengths of the ligand-centered transitions induces photodecarboxylation (eq 4).[1]

$$fac\text{-}(RCO_2)Re^I(CO)_3(2,2'\text{-bpy}) + h\nu \rightarrow {}^3LLCT \rightarrow R^\bullet + CO_2 + Re(CO)_3(2,2'\text{-bpy})^+ \quad (4)$$

The reaction appears to be initiated, however, in a long-lived ligand-to-ligand charge transfer (LLCT) excited state. In contrast to the case for *fac*-(4-nitrobenzylCO_2)$Re^I(CO)_3$(2,2′-bpy), $^3MLCT_{Re\rightarrow RCO_2}$ excited states must have been produced in very low concentrations when *fac*-$(RCO_2)Re^I(CO)_3$(2,2′-bpy) (R =

---

* To whom correspondence should be addressed. E-mail: ferraudi.1@nd.edu (G.F.); mfeliz@inifta.unlp.edu.ar (M.R.F.).

[†] Universidad Nacional de La Plata.

[‡] University of Notre Dame.

[§] Universidad de Santiago. E-mail: jguerrero@usach.cl.

(1) Wolcan, E.; Torchia, G.; Tocho, J.; Piro, O. E.; Juliarena, P.; Ruiz, G.; Feliz, M. R. *Dalton Trans.* **2002**, 2194.

(2) Glazeen, M. M.; Lees, A. *J. Am. Chem. Soc.* **1988**, *110*, 3892, 6243.

(3) Ruiz, G. T.; Juliarena, M. P.; Lezna, R. O.; Wolcan, E.; Féliz, M. R.; Ferraudi. G. *Helv. Chim. Acta* **2002**, *85*, 1261.

(4) MacQueen, D. B.; Schanze, S. K. *J. Am. Chem. Soc.* **1991**, *113*, 7470.

(5) Busby, M.; Gabrielsson, A.; Matosek, P.; Towrie, M.; Di Bilio, A. J.; Gray, H. B.; Vlček, A., Jr. *Inorg. Chem.* **2004**, *43*, 4994.

(6) Feliz, M. R.; Ferraudi, G. *Inorg. Chem.* **1998**, *37*, 2806.

(7) Ronco, S.; Ferraudi, G. In *Handbook of Photochemistry and Photobiology*; Nalwa, H. S., Ed.; American Scientific: Stevenson Ranch, CA, 2003; Vol. 1, Chapter 8, and references therein.

(8) Kleverlaan, C. J.; Stufkens, D. J.; Clark, I. P.; George, M. W.; Turner, J. J.; Martino, D. M.; van Willegen, H.; Vlček, A., Jr. *J. Am. Chem. Soc.* **1998**, *120*, 10871.

(9) Guerrero, J.; Piro, O. E.; Wolcan, E.; Feliz, M. R.; Ferraudi, G.; Moya, S. A. *Organometallics* **2001**, *20*, 2842.

10.1021/om0604775 CCC: $37.00

methyl, 1-pyrenyl, 9-anthranyl, 2-naphthyl) complexes were irradiated at wavelengths of the IL and charge transfer absorption bands.

A probable cause of the disparate photobehavior of these carboxylate complexes must be the different rates of the processes populating $^3MLCT_{Re\rightarrow 2,2'-bpy}$, $^3MLCT_{Re\rightarrow RCO_2}$, and LLCT excited states. While $^3MLCT_{Re\rightarrow 4-O_2NC_6H_4CO_2}$ in *fac*-(4-nitrobenzylCO_2)$Re^I(CO)_3$(2,2′-bpy) is rapidly populated, the LLCT excited states in *fac*-(RCO_2)$Re^I(CO)_3$(2,2′-bpy) (R = alkyl, aryl) are those being preferentially populated by the relaxation of the Franck−Condon excited state. Although the R groups appear to be electronically insulated from the Re^I-$(CO)_3$Y chromophore, the disparity in the photophysics of the complexes was the result of differences in the electron-donating/-withdrawing characters of the R groups in the ligands RCO_2^-. The 4-nitrobenzyl group has a strongly electron withdrawing character while R = alkyl, aryl vary from being weakly electron withdrawing to weakly electron donating groups.

The complexes *fac*-(RCO_2)$Re^I(CO)_3$(2,2′-bpy), where R is a strong electron donor, are expected to have LLCT excited states at much lower energies than the previously studied carboxylate complexes.[1,3,9] A photochemical behavior, different from that previously showed by *fac*-(RCO_2)$Re^I(CO)_3$(2,2′-bpy) (R = alkyl, aryl) can be expected in complexes having such low-lying LLCT excited states. Two R groups with strong electron-donating properties are ferrocene and 4-DMAB (4-DMAB = 4-(dimethylamino)benzyl). While low-energy metal-centered states could be available in the ferrocene group for the degradation of the MLCT and LLCT Franck−Condon excited-state energies, no such excited states are available in 4-DMAB. Given these differences between ferrocene and 4-DMAB and between these groups and those with R = alkyl, aryl, the photophysical and photochemical properties of *fac*-(RCO_2)$Re^I(CO)_3$L (R = 4-DMAB, L = phen, (I); R = ferrocene; L = phen, (II), 2,2′-bpy, (III)) were investigated in this work.

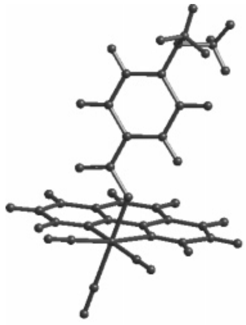
(I)

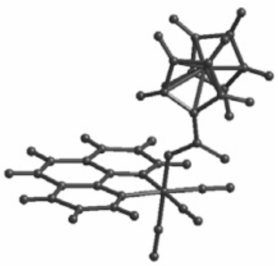
(II)

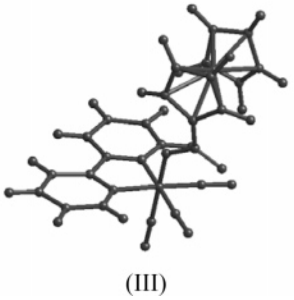
(III)

Experimental Section

All of the experiments described here were conducted with deaerated solutions kept at room temperature. Other experimental procedures and apparatus are described next.

Flash Photochemical Procedures. Absorbance changes, ΔA, occurring on a time scale longer than 10 ns were investigated with a flash photolysis apparatus described elsewhere.[9−11] In these experiments, 10 ns flashes of 351 nm light were generated with a Lambda Physik SLL-200 excimer laser. The energy of the laser flash was attenuated to values equal to or less than 20 mJ/pulse by absorbing some of the laser light in a filter solution of $Ni(ClO_4)_2$ with the desired optical transmittance, $T = I_t/I_0$, where I_0 and I_t are respectively the intensities of the light arriving to and transmitted from the filter solution. The transmittance, $T = 10^{-A}$, was routinely calculated by using the spectrophotometrically measured absorbance, A, of the filter solution. A right-angle configuration was used for the pump and probe beams. Concentrations of the Re complexes were adjusted to provide homogeneous concentrations of photogenerated intermediates over the optical path, $l = 1$ cm, of the probe beam. To satisfy this optical condition, solutions were made with an absorbance equal to or less than 0.8 over the 0.2 cm optical path of the pump.

A CPA-2010 1 kHz amplified Ti:sapphire laser system from Clark MXR and software from Ultrafast Systems were used for the observation of transient absorption spectra and the study of reaction kinetics in a femtosecond to 1.6 ps time domain. The flash photolysis apparatus provides 775, 387, or 258 nm laser pulses for excitation with a pulse width of 150 fs. Data points can be collected at intervals equal to or longer than 10 fs. A slow but constant flow of the solutions through a 2 mm cuvette was maintained during the photochemical experiments.

Time-resolved fluorescence experiments were carried out with a PTI flash fluorescence instrument. The excitation light was provided by a N_2 laser ($\lambda_{em} = 337$ nm, ca. 2 mJ/pulse and 200 ps bandwidth at half-height). All the solutions used in the photochemical work were deaerated for $^1/_2$ h with streams of ultrahigh-purity N_2 before and during the irradiations.

The fitting of data to analytical functions was made with commercially available routines, MicroCal Origin 6 and Mathcad 8. The routines for the fittings used a nonlinear least-squares method, and the goodness of the fits was established by the χ^2, standard, and quadratic deviations.

Steady-State Irradiations. The luminescence of the compounds was investigated in a Perkin-Elmer LS 50B spectrofluorometer by procedures reported elsewhere.[1,3,9,12] The spectra were corrected for differences in instrumental response and light scattering. Solutions were deaerated with ultrahigh-purity N_2 in a gastight apparatus before recording the spectra.

Equation 5 was used for the calculation of the quantum yield of emission, ϕ_{LUM}, by using solutions of a reference compound with a known quantum yield of emission, $\phi(\mathrm{ref})_{LUM}$.

$$\phi_{LUM} = \frac{I_{Re}}{I_{ref}}\frac{A_{ref}}{A_R}\left(\frac{n_{Re}}{n_{ref}}\right)^2\phi(\mathrm{ref})_{LUM} \qquad (5)$$

In eq 5, n_{Re} and n_{ref} are respectively the refractive indexes of the optically diluted solutions of the Re complex and reference compounds: i.e., solutions with A_{ref} and $A_{Re} < 0.1$. A solution of Rhodamine B in ethanol was used as a reference with $\phi(\mathrm{ref})_{LUM} = 0.69$. The areas under the emission spectra of the Re(I) complexes and Rhodamine B were used as relative measures of the respective intensities of the luminescence, I_{Re} and I_{ref}.[13]

A literature procedure was used in order to verify that radiative relaxations of more than one excited state contributed to the

---

(10) Feliz, M. R.; Ferraudi, G.; Altmiller. H. J. *J. Phys. Chem.* **1992**, *96*, 257.

(11) Feliz, M. R.; Ferraudi, G. *J. Phys. Chem.* **1992**, *96*, 3059.

(12) Feliz, M. R.; Rodriguez Nieto, F.; Ruiz, G.; Wolcan, E. *J. Photochem. Photobiol. A: Chem.* **1998**, *117*, 185.

(13) Scaiano, J. C. *Handbook of Photochemistry*; CRC Press: Boca Raton, FL, 1989; Vol. 1.

luminescence.[14] In this procedure, two uncorrected excitation spectra were measured with the same solution of Re(I) complex. The luminescence was investigated at two different wavelengths, $\lambda_{obs,1}$ and $\lambda_{obs,2}$. The calculated parameter is $\rho(\lambda)$: i.e., the quotient between the intensities of the luminescence, $\rho(\lambda_{exc}) = I(\lambda_{obs,1})/I(\lambda_{obs,2})$, at the wavelength of the excitation, λ_{exc}. A contribution from a single source makes $\rho(\lambda_{exc})$ independent of λ_{exc}.

Steady-state irradiations of the Re(I) complexes in deaerated solutions were carried out with light from a 300 or a 350 nm Rayonet lamp. The solutions for these experiments were placed in a dual reaction cell with 1 and 0.2 cm optical paths. The cell has been described elsewhere in the literature.[15] Concentrations of Re(I) complexes equal to or larger than 1.0×10^{-4} M were used in the side with the 1 cm optical path in order to absorb all the incident light during the photolysis. The optical changes induced by the irradiation were investigated with the solution displaced to the chamber with the 0.2 cm optical path. Light intensities communicated elsewhere in the text were measured with Parker's actinometer.[16]

Electrochemical Measurements. A PAR Model 173 potentiostat with a 276A interface module and a Model 175 universal programmer were used for dc and ac voltammetry.[17−20] Acetonitrile (Merck "SecoSolv") was dried further over activated alumina for several days. The procedure was found to be suitable for electrochemistry in the −1.5 to +0.6 V potential range. Bu_4NPF_6 was dried under vacuum at 80 °C for at least 24 h. A 0.1 M concentration of Bu_4NPF_6 was used as supporting electrolyte. Platinum disks, polished to a mirror finish, were used as working electrodes. Potentials were measured against a $Ag/AgCl/KCl_{sat}$ electrode. Oxygen was removed by bubbling purified N_2 for at least 30 min prior to each experiment.

Pulse Radiolytic Procedures. Pulse radiolysis experiments were carried out with a Model TB-8/16-1S electron linear accelerator. The instrument and computerized data collection for time-resolved UV−vis spectroscopy and reaction kinetics have been described elsewhere in the literature.[21,22] Thiocyanate dosimetry was carried out at the beginning of each experimental session. The details of the dosimetry have been reported elsewhere.[6,21−25] The procedure is based on the concentration of $(SCN)_2^-$ radicals generated by the electron pulse in a N_2O-saturated 10^{-2} M SCN^- solution. In the procedure, the calculations were made with $G = 6.13$ and the extinction coefficient $\epsilon = 7.58 \times 10^3$ M^{-1} cm^{-1} at 472 nm for the $(SCN)_2^-$ radicals.[22,23] In general, the experiments were carried out with doses that in N_2-saturated aqueous solutions resulted in $(2.0 \pm 0.1) \times 10^{-6}$ to $(6.0 \pm 0.3) \times 10^{-6}$ M concentrations of e^-_{sol}. In these experiments, solutions were prepared by the procedure indicated above for the photochemical experiments. The liquids were deaerated with streams of the O_2-free gas, N_2 or N_2O, that was required for the experiment. In order to radiolyze a fresh sample with each pulse, an appropriate flow of the solution through the reaction cell was maintained during the experiment. Other conditions used for the time-resolved spectroscopy of the reaction intermediates or in the investigation of the reaction kinetics are given in the Results. Radiolyses with ionizing radiation of CH_3OH and CH_3OH/H_2O mixtures have been reported elsewhere in the literature.[22,24,25] These studies have shown that pulse radiolysis can be used as a convenient source of e^-_{sol} and $C^{\bullet}H_2OH$ radicals (Scheme 1).

Scheme 1

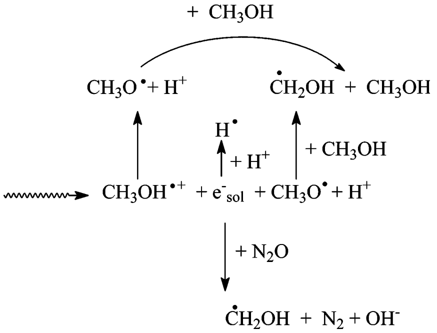

Since e^-_{sol} and $C^{\bullet}H_2OH$ have large reduction potentials, i.e., $E° \approx -2.8$ V vs NHE for e^-_{sol} and $E° \approx -0.92$ V vs NHE for $C^{\bullet}H_2OH$, they have been used for the reduction of coordination complexes and for the study of electron-transfer reactions. The yield of e^-_{sol} in CH_3OH ($G \approx 1.1$),[24] is about one-third of the G value in the radiolysis of H_2O ($G \approx 2.8$).[25] In solutions where e^-_{sol} was scavenged with N_2O, the $C^{\bullet}H_2OH$ radical appears to be the predominant product (yield >90%) of the reaction between CH_3OH and $O^{\bullet -}$.

Materials. Literature procedures were used for the preparations of *fac*-$(CF_3SO_3)Re^I(CO)_3$(2,2′-bpy),[26,27] *fac*-$(CF_3SO_3)Re^I(CO)_3$(phen),[26,27] *fac*-$(CH_3CO_2)Re^I(CO)_3$(phen),[1] and *fac*-$(CH_3CO_2)Re^I(CO)_3$(2,2′-bpy).[28] The UV−vis and IR spectra of these complexes compared very well with those already communicated in the literature.

***fac*-(4-DMABCO$_2$)Re^I(CO)$_3$(phen) (I).** 4-DMABCO$_2$H (0.040 g) and 0.244 cm^3 of a 1 M solution of tetrabutylamonium hydroxide in methanol were dissolved in 10 cm^3 of absolute ethanol and kept standing for 15 min. This solution and *fac*-$(CF_3SO_3)Re^I(CO)_3$(phen) (0.160 g) were added to 100 cm^3 of ethanol. The solution was brought to reflux after being deaerated with N_2, and the reflux of the liquid under N_2 was maintained for 7 h. A solid, obtained by the rotavaporation of the solvent, was recrystallized from 15 cm^3 of CH_2Cl_2 by the addition of chilled isooctane. Two recrystallizations from CH_2Cl_2 were made by the same procedure. The pure product (yield 80%) was dried under vacuum. Anal. Calcd: C, 46.89; N, 6.80; H, 2.99. Found: C, 46.70; N, 6.70; H, 2.94.

***fac*-(ferroceneCO$_2$)Re^I(CO)$_3$(phen) (II).** ferroceneCOOH (0.068 g) and 0.296 cm^3 of a 1 M solution of tetrabutylamonium hydroxide in methanol were mixed in 10 cm^3 of ethanol and stirred for 15 min. A solution containing 0.177 g of *fac*-$(CF_3SO_3)ReCO_3$(phen) in 150 cm^3 of ethanol was added to the previous solution, and the liquid was brought to reflux after being deaerated with N_2. The reflux of the liquid under N_2 was maintained for 12 h. An orange solid precipitated after chilling the solution. The solid was filtered and dissolved in the minimum volume of CH_2Cl_2. A pure product was obtained by the slow addition of chilled isooctane. The pure product (yield 70%) was dried under vacuum. Anal. Calcd: C, 45.96; N, 4.12; H, 2.52. Found: C, 45.88; N, 4.12; H, 2.50.

***fac*-(ferroceneCO$_2$)Re^I(CO)$_3$(2,2′-bpy) (III).** ferroceneCOOH (0.176 g) and 0.76 cm^3 of a 1 M solution of tetrabutylamonium

---

[14] Demas, J. N. *Excited State Lifetime Measurements*; Academic Press: New York, 1983.

[15] Ferraudi, G. *Inorg. Chem.* **1980**, *19*, 438.

[16] Hatchard, C. G.; Parker, C. A. *Proc. R. Soc. London, Ser. A* **1956**, *235*, 518.

[17] Lezna, R. O. *An. Asoc. Quím. Argent.* **1988**, *76*, 25−44.

[18] Lezna, R. O. *An. Asoc. Quím. Argent.* **1994**, *82*, 293.

[19] Southampton Electrochemistry Group. *Instrumental Methods in Electrochemistry*; Ellis Horwood: Chichester, U.K., 1985.

[20] Lezna, R. O.; Juanto, S.; Zagal, J. H. *J. Electroanal. Chem.* **1995**, *389*, 197.

[21] Buxton, G. V.; Greenstock, C. L.; Hellman, W. P.; Ross, A. B.; Tsang, W. *J. Phys. Chem. Ref. Data* **1988**, *17*, 513.

[22] Getoff, N.; Ritter, A.; Schworer, F. *Radiat. Phys. Chem.* **1993**, *41*, 797.

[23] Hugh, G. L.; Wang, Y.; Schöneich, C.; Jiang, P.-Y.; Fesenden, R. W. *Radiat. Phys. Chem.* **1999**, *54*, 559.

[24] Dorfman, L. M. In *The Solvated Electron in Organic Liquids*; Gould, R. F., Ed.; Advances in Chemistry Series; American Chemical Society: Washington, DC, 1965.

[25] Simic, M.; Neta, P.; Hayon, E. *J. Phys. Chem.* **1969**, *73*, 3794.

[26] Schanze, K. S.; MacQueen, D. B.; Perkin, T. A.; Cabana, L. A. *Coord. Chem. Rev.* **1993**, *122*, 63.

[27] Caspar, J. V.; Sullivan, B. P.; Meyer, T. J. *Organometallics* **1983**, *2*, 551.

[28] Juliarena, M. P. Ph.D. Dissertation, University of La Plata, 2005.

Table 1. Quantum Yield, ϕ, for the Photoinduced Photodecarboxylation of Re(I) Complexes Irradiated at 300 nm[a]

	φ
fac-(4-DMABCO$_2$)Re^I(CO)$_3$(phen)[b]	5.3×10^{-4}
fac-(ferroceneCO$_2$)Re^I(CO)$_3$(phen)[b]	1.4×10^{-3}
fac-(ferroceneCO$_2$)Re^I(CO)$_3$(2,2′-bpy)[c]	1.1×10^{-3}
fac-(CH$_3$CO$_2$)Re^I(CO)$_3$(phen)	1.0×10^{-2}
fac-(CH$_3$CO$_2$)Re^I(CO)$_3$(2,2′-bpy)[c]	1.7×10^{-2}

[a] The complexes were irradiated in deaerated CH_3CN and the reaction was followed by means of the absorbance change at λ_{obs}. Other petrochemical conditions are indicated elsewhere in the text. [b] Reaction followed at λ_{obs} 365 nm. [c] Reaction followed at λ_{obs} 315 nm.

hydroxide in methanol were mixed in 50 cm^3 of ethanol and stirred 15 min. A solution containing 0.434 g of *fac*-(CF$_3$SO$_3$)ReCO$_3$(2,2′-bpy) in 250 cm^3 of ethanol was added to the previous solution, and the liquid was brought to reflux after being deaerated with N_2. The reflux of the liquid under N_2 was maintained for 12 h. A yellow solid precipitated after chilling the solution. The solid was filtered and dissolved in the minimum volume of CH_2Cl_2. A pure product was obtained by the slow addition of chilled isooctane. The pure product (yield 70%) was dried under vacuum. Anal. Calcd: C, 43.98; N, 4.27; H, 2.61. Found: C, 43.97; N, 4.20; H, 2.64.

The compounds I–III were characterized by means of IR (Figured 1S–3S, Supporting Information) and NMR spectra (Figures 4S–6S, Supporting Information). Other materials were reagent grade and were used without further purification.

Results

Photolyses of *fac*-(RCO$_2$)Re^I(CO)$_3$L (R = ferrocene, L = phen, 2,2′-bpy; R = 4-DMAB, L = phen) in CH_3CN or CH_2Cl_2 were carried out at 300 nm. For the sake of brevity, these complexes will be designated *fac*-(RCO$_2$)Re^I(CO)$_3$L in the following paragraphs unless explicitly indicated. The *fac*-(RCO$_2$)Re^I(CO)$_3$L complexes underwent the photodecarboxylation process (eq 4) previously communicated for the photolysis of *fac*-(CH$_3$CO$_2$)Re^I(CO)$_3$L (L = 2,2′-bpy).[1] In order to compare the rates of photodecarboxylation under similar optical conditions, i.e., conditions ensuring that 99.9% of the incident light at 300 nm was absorbed during the entire length of the photolysis, solutions of the *fac*-(RCO$_2$)Re^I(CO)$_3$L complexes with an absorbance equal to or greater than $A \geq 2.25$ at 300 nm were photolyzed with an intensity of the incident light, $I_0 \approx 4 \times 10^{-4}$ einstein dm^{-3} s^{-1}. Spectral changes in the 200–500 nm region of the solutions' absorption spectra were recorded as a function of the irradiation period. On the basis of the rates of spectral change, the photodecarboxylations of *fac*-(RCO$_2$)Re^I(CO)$_3$L were more than 10 times slower than the processes of the reference complexes, *fac*-(CH$_3$CO$_2$)Re^I(CO)$_3$L (Table 1).

No spectral changes were observed in the UV–vis absorption spectra of solutions containing 10^{-5}, 4.2×10^{-4}, or 3×10^{-3} M *fac*-(RCO$_2$)Re^I(CO)$_3$L in CH_3CN or CH_2Cl_2 when they were photolyzed at $\lambda_{exc} = 350$ nm: i.e., a wavelength associated with Re to L charge-transfer transitions. The spectral changes remain insignificant when the irradiations were carried out for periods as long as 24 h. This experimental observation is in agreement with the stability toward photodecarboxylation shown by *fac*-(RCO$_2$)Re^I(CO)$_3$L (R = alkyl, aryl) when they were irradiated at wavelengths of the MLCT transitions.

The photophysical reasons for the differences between the photoreactivity of *fac*-(RCO$_2$)Re^I(CO)$_3$L and the reference complexes were investigated with various steady-state and time-resolved spectroscopic methods.

Absorption Spectroscopy and Redox Potentials. The UV–vis absorption spectra of *fac*-(RCO$_2$)Re^I(CO)$_3$L were recorded as a function of complex concentration in CH_3CN or CH_2Cl_2. Intense absorption bands in the UV–vis absorption spectra of *fac*-(RCO$_2$)Re^I(CO)$_3$L complexes, similar to those observed in the spectra of related Re(I) complexes, must be assigned to electronic transitions from the ^{1}A ground state to IL and MLCT$_{Re\to L}$ excited states (Table 2).[7,29,30] Absorption bands due to IL transitions have maxima at wavelengths equal to or shorter than 350 nm. Other intense absorption bands, associated with MLCT$_{Re\to L}$ transitions, have maxima at $\lambda_{max} > 350$ nm, in accordance with the redox potentials of the Re(II)/Re(I) and L/L$^{\bullet-}$ couples (Table 2). The position of the MLCT bands shifts toward shorter wavelengths with the dielectric constant of the solvent. A similar medium effect has been communicated in the literature for related Re(I) complexes.[31,32] In addition, the increase of the absorbance with complex concentration in CH_3CN or CH_2Cl_2 follows Beer's law at wavelengths of the MLCT and intraligand (IL) absorption bands. This experimental observation shows that no oligomers are formed when the concentration of complex is equal to or smaller than 10^{-4} M.

On the basis of the redox potentials of the $RCO_2^{\bullet}/RCO_2^-$ and L/L$^{\bullet-}$ couples in Table 2, absorption bands due to optically induced RCO_2^- to L charge-transfer transitions, LLCT, were expected to be placed at $\lambda > 560$ nm. However, these LLCT$_{RCO_2\to L}$ electronic transitions are weak, due to the small orbital overlap.[7] Observation in the spectrum of the complexes was precluded by the small extinction coefficients of absorption bands associated with such electronic transitions. Also on the basis of the redox potentials in Table 2, a singlet excited state involving a transfer of charge from the Re to a coordinated carboxylate group, i.e., ^{1}MLCT$_{Re\to RCO_2}$, should be placed at $\lambda_{max} \sim 370$ nm. An unequivocal identification of absorption bands associated with ^{1}MLCT$_{Re\to RCO_2} \leftarrow {}^1$A electronic transitions could not be made from the inspection of the complexes' absorption spectrum.

Steady-State Luminescence. Deaerated solutions of *fac*-(ferroceneCO$_2$)Re^I(CO)$_3$(phen) with concentrations of the complex equal to or less than 8.8×10^{-5} M in CH_3CN were irradiated at 337, 350, or 400 nm to record the emission spectrum. The band gradually changed shape, and the intensity decreased with increasing complex concentration (Figure 1). Stern–Volmer plots were constructed for two excitation wavelengths, i.e., λ_{exc} 337 and 400 nm, and two monitoring wavelengths, i.e., λ_{obs} 525 and 600 nm (inset to Figure 1). Differences between the Stern–Volmer constants, K_{SV}, calculated from the slopes of these linear plots were larger than the error, $\delta K_{SV} \leq 10\%$, affecting the values of K_{SV} (Table 3). This dependence of the *fac*-(ferroceneCO$_2$)Re^I(CO)$_3$(phen) luminescence on complex concentration is consistent with more than one excited state undergoing a radiative relaxation to the ground state. In addition, the self-quenching of their different contributions to the overall emission spectrum must occur with different rates which give rise to the dependence of K_{SV} on the monitoring wavelength (Table 3).

In the self-quenching of the emission, the role of the quencher can be attributed to the ferroceneCO$_2^-$ ligand of the *fac*-(ferroceneCO$_2$)Re^I(CO)$_3$(phen) complex. It is expected, therefore, that additions of ferroceneCO$_2^-$ to solutions of *fac*-

---

(29) Revill, J. A. T.; Brown, R. G. *J. Fluoresc.* **1992**, *2*, 107.

(30) Fery-Forgues, S.; Delavaux-Nicot, B. *J. Photochem. Photobiol. A: Chem.* **2000**, *132*, 137.

(31) Ronco, S.; Ferraudi, G. In *Handbook of Photochemistry and Photobiology*; Nalwa, H. S., Ed.; American Scientific: Stevenson Ranch, CA, 2003; Vol. 1, Chapter 8, pp 316–318, and references therein.

(32) Stufkens, D. J.; Vlček, A., Jr. *Coord. Chem. Rev.* **1998**, *177*, 127 and references therein.

Table 2. Assignment of Absorption Bands and Redox Couples of *fac*-(RCO_2)$Re^I(CO)_3L$ Complexes and Relevant Ligands

R	L	λ_{max},[a] nm (ϵ, 10^3 M^{-1} cm^{-1}) [assign][b]	E°, V (vs NHE)[c]			
			$RCO_2^{\bullet}/RCO_2^-$	Re^{II}/Re^I	L/L$^-$	$RCO_2^-/RCO_2^{\bullet 2-}$
ferrocene	phen	380 (5.2) [$\pi^* \leftarrow d\pi$]	0.71	1.53	−0.74[d]	
		290 (17.1) [$\pi^* \leftarrow \pi$]			−1.08	
		268 (36.2) [$\pi^* \leftarrow \pi$]				
	2,2′-bpy	386 (3.2) [$\pi^* \leftarrow d\pi$]	0.74	1.54	−1.14	
		292 (16.8) [$\pi^* \leftarrow \pi$]			−1.45	
		242 (21.0) [$\pi^* \leftarrow \pi$]				
		<220 [$\pi^* \leftarrow \pi$]				
4-DMAB	phen	380 (2.8) [$\pi^* \leftarrow d\pi$]	1.11	1.67	−1.08	
		290 (23.5) [$\pi^* \leftarrow \pi$]				
		270 (24.7) [$\pi^* \leftarrow \pi$]				
ferroceneCO_2H[e]		440 (0.26) [d ← d]	0.87			
		310 (1.1) [d ← d]				
		262 (5.1) [$\pi^* \leftarrow d\pi$]				
		<220 (>10) [$\pi^* \leftarrow d\pi$]				
CH_3CO_2H		205 (0.046)[f] [$\pi^* \leftarrow \pi$]	~2.1			−1.8[g]
4-DMABCO_2^- [h]		316 (30.0) [$\pi^* \leftarrow \pi$]	1.15			
		232				

[a] Wavelength of the maxima observed in the spectra of solutions made in CH_2Cl_2. [b] Assignments: $\pi^* \leftarrow d\pi$ electronic transition populating $^1MLCT_{Re \rightarrow L}$ excited states, $\pi^* \leftarrow \pi$ electronic transition populating ^1IL excited states of L or RCO_2^-. [c] Redox potentials were determined in CH_3CN vs a AgCl(sat)/Ag reference electrode (see the Experimental Section). These values of E° were referenced to the NHE by adding the potential of the reference electrode: $E° \approx 0.197$ V vs NHE. All are reversible couples unless explicitly indicated. [d] Irreversible. [e] Assignment of electronic transitions from ref 30. [f] In H_2O. [g] The reduction of RCO_2^- in *fac*-(CH_3CO_2)$Re^I(CO)_3L$ is seen as an irreversible wave at −1.52 V vs NHE. Similar processes were observed between this potential and the CH_3CO_2H potential in the table for R = naphthyl, anthracenyl, pyrenyl.[1] [h] Assignment of electronic transitions from ref 29.

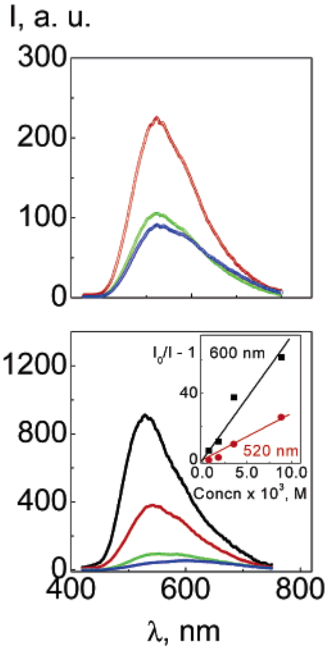

Figure 1. Concentration dependence of the *fac*-(ferroceneCO_2)-$Re^I(CO)_3$(phen) emission spectrum: (top) λ_{exc} 337 nm; (bottom) λ_{exc} 400 nm. The concentrations of the complex in CH_3CN are 7.0×10^{-6} M (black), 1.8×10^{-5} M (red), 3.5×10^{-5} M (green), 8.8×10^{-5} M (blue). The inset shows Stern−Volmer plots for the autoquenching of the luminescence at λ_{obs} 600 nm (■) and 520 nm (●).

(ferroceneCO_2)$Re^I(CO)_3$(phen) will also quench the luminescence. This effect was investigated with ~8×10^{-6} M solutions of *fac*-(ferroceneCO_2)$Re^I(CO)_3$(phen) in CH_3CN containing concentrations of ferroceneCO_2^- between 1.7×10^{-5} and 8.8×10^{-5} M. The Stern−Volmer plots were fairly linear, and the values of K_{SV} calculated from the slopes of the lines (Table 3) were smaller than those of the self-quenching processes. This difference between K_{SV} values suggests that the self-quenching proceeds via static and dynamic pathways, while only a dynamic quenching operates when ferroceneCO_2^- is the quencher. Due to the low intensity of the luminescence, we were unable to conduct similar quenching experiments with *fac*-(ferroceneCO_2)-$Re^I(CO)_3$(2,2′-bpy).

Table 3. Quantum Yields (ϕ_{LUM}) and Lifetimes (τ_{LUM}) of the *fac*-(RCO_2)$Re^I(CO)_3L$ Complexes' Luminescence and Rate Constants (k_q) and Stern−Volmer Constants (K_{SV}) for the Autoquenching of the Luminescence and Quenching by ferroceneCO_2H[a]

λ_{exc}, nm	ϕ_{LUM}[b]	τ_{LUM}, ns	k_q, M^{-1} s^{-1}	K_{SV}, M^{-1}	
		fac-(ferroceneCO_2)$Re^I(CO)_3$(phen)			
400	5.8×10^{-4} [c]				
	5.5×10^{-5}			2.8×10^5 [g]	7.5×10^5 [h]
350	5.9×10^{-4} [c]				
	3.9×10^{-4}				
337	5.9×10^{-4} [c]	80, 800[c]	2.5×10^{10} [c]		
	4.0×10^{-4}	155, 2700	1.4×10^{10}	1.3×10^5 [g]	2.3×10^5 [h]
		fac-(ferroceneCO_2)$Re^I(CO)_3$(2,2′-bpy)			
400	1.0×10^{-4} [c]				
	5.7×10^{-5}				
350	1.4×10^{-4}				
337	1.2×10^{-4} [c]	80, 650[c]			
	1.5×10^{-4}	30, 380	8.8×10^9		
		fac-(4-DMABCO_2)$Re^I(CO)_3$(phen)			
400	*d*		*d*	3.1×10^4 [i]	5.0×10^4 [h]
337	*d*	3, 25	*d*	3.1×10^4 [i]	3.1×10^4 [h]
		fac-(CH_3CO_2)$Re^I(CO)_3$(phen)			
400	2.7×10^{-3} [c,e]				
	7.1×10^{-4} [e]	27, 248			
350	2.5×10^{-3} [c,e]				
	1.4×10^{-3} [e]				
337	2.2×10^{-3} [c,e]				
	1.5×10^{-3} [c,e]				
		fac-(CH_3CO_2)$Re^I(CO)_3$(2,2′-bpy)			
350	4.0×10^{-3} [c,f]	31, 244[c,f]			
337	1.1×10^{-3} [f]	474[f]			
		fac-(ferroceneCO_2)$Re^I(CO)_3$(phen)/ferroceneCO_2H			
400				8.1×10^4	2.7×10^4
337				9.2×10^4	5.6×10^4

[a] In CH_3CN unless otherwise indicated. [b] For *fac*-(CH_3CO_2)$Re^I(CO)_3$(phen), $\tau_{LUM} = 474$ ns and $\phi_{LUM} = 1.1 \times 10^{-3}$ in CH_3CN. In CH_2Cl_2, $\phi = 4.0 \times 10^{-3}$. [c] In CH_2Cl_2. [d] Emission too weak to be determined. [e] Data from ref 28. [f] Data from ref 1. [g] λ_{obs} 520 nm. [h] λ_{obs} 600 nm. [i] λ_{obs} 537 nm.

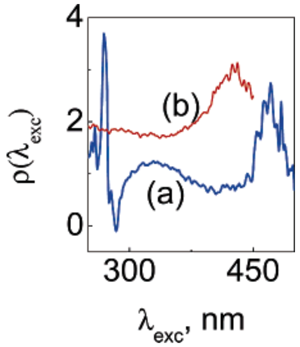

Figure 2. Dependence of the ratio $\rho = I(\lambda_1)_{LUM}/I(\lambda_2)_{LUM}$ of two excitation spectra recorded by monitoring the luminescence at two different wavelengths. In (a), the excitation spectra of *fac*-(ferroceneCO$_2$)Re^I(CO)$_3$(phen) in CH$_3$CN were recorded using λ_1 520 nm and λ_2 580 nm. The excitation spectra of *fac*-(ferroceneCO$_2$)-Re^I(CO)$_3$(2,2′-bpy) in CH$_2$Cl$_2$ (b) were recorded using λ_1 530 nm and λ_2 580 nm.

In contrast to the luminescence spectrum of *fac*-(ferroceneCO$_2$)-Re^I(CO)$_3$L in CH$_3$CN, the emission spectrum in CH$_2$Cl$_2$ exhibits a symmetric, broad band at λ_{max} ~610 nm that is nearly independent of the excitation wavelength (λ_{exc} 337, 400 nm) and concentration of complex ([complex] $\leq 8.8 \times 10^{-5}$ M).

The dependencies of the *fac*-(4-DMABCO$_2$)Re^I(CO)$_3$(phen) emission spectrum on solvent, complex concentration, and λ_{exc} value are similar to those described above for the *fac*-(ferroceneCO$_2$)Re^I(CO)$_3$L complexes. The low intensity of the complex luminescence did not allow the accurate determination of K_{SV} when the emission was quenched by increasing concentrations of 4-DMABCO$_2$H.

Evidence for the overlap of components in the emission spectrum of *fac*-(ferroceneCO$_2$)Re^I(CO)$_3$L was also found in the excitation spectrum. In order to minimize the effect of self-quenching, the excitation spectrum was recorded with ~8×10^{-6} M concentration of the complexes. Quotients, $\rho(\lambda_{exc})$, of two excitation spectra, recorded with the same solution of the complex and two different monitoring wavelengths, $\lambda_{obs,1}$ and $\lambda_{obs,2}$, were strongly dependent on λ_{exc} (Figure 2).

The luminescence quantum yields, ϕ_{LUM}, measured with *fac*-(RCO$_2$)Re^I(CO)$_3$(2,2′-bpy) complexes in CH$_3$CN or CH$_2$Cl$_2$ (Table 3) were ~30 times smaller than those literature values communicated for *fac*-(CH$_3$CO$_2$)Re^I(CO)$_3$(2,2′-bpy). Quantum yields for the luminescence of *fac*-(RCO$_2$)Re^I(CO)$_3$(phen) were ~3 times smaller than the luminescence yield of *fac*-(CH$_3$CO$_2$)-Re^I(CO)$_3$(phen).

Time-resolved emission and absorption spectroscopy was used for a study of the photoprocesses associated with the luminescence of the Re(I) complexes.

Time-Resolved Emission Spectroscopy. In these experiments, the luminescence of *fac*-(RCO$_2$)Re^I(CO)$_3$L complexes was investigated as a function of solvent, i.e., CH$_3$CN or CH$_2$Cl$_2$, and complex concentration. A biexponential decay of the luminescence, A_{fast} exp $-t/\tau_{fast} + A_{slow}$ exp $-t/\tau_{slow}$, accounts for the decay of the luminescence. Emission spectra associated with these components of the luminescence are shown in Figure 3, and the corresponding lifetimes are communicated in Table 3. The lifetime of the slow component decreased with complex concentration as a result of the self-quenching described above. Plots of $1/\tau_{slow}$ vs complex concentration were linear and rate constants, k_q, of the self-quenching reactions (Table 3) were calculated from the slopes of the lines. In CH$_2$Cl$_2$, the rate constants of the *fac*-(ferroceneCO$_2$)Re^I(CO)$_3$L complexes are $k_q = 2.5 \times 10^{10}$ M^{-1} s^{-1} for L = phen and $k_q = 8.8 \times 10^9$ M^{-1} s^{-1} for L = 2,2′-bpy. In CH$_3$CN, $k_q = 1.4 \times 10^{10}$ M^{-1} s^{-1} for L = phen.

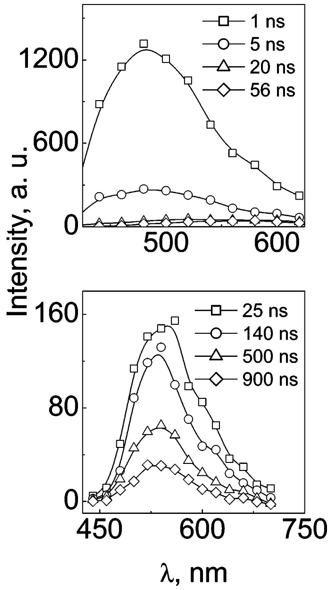

Figure 3. Time-resolved emission spectra of *fac*-(RCO$_2$)Re^I(CO)$_3$-(phen): (top) R = 4-DMAB; (bottom) R = ferrocene. Deaerated solutions of the Re(I) complexes in CH$_3$CN were flash-irradiated at 337 nm. Keys to the delays from the flash irradiation are given in the figure.

Time-Resolved Absorption Spectroscopy. Transient absorption spectra in the femtosecond to nanosecond and in the 15 ns to microsecond time domains were recorded with two flash photolysis instruments, providing respectively 387 and 351 nm laser pulses for the irradiation of the complexes. In order to minimize the effect of reactions between the ground and excited states of the complexes at times longer than 10 ns, deaerated solutions with concentrations equal to or smaller than 8×10^{-6} M in *fac*-(RCO$_2$)Re^I(CO)$_3$L in CH$_3$CN or CH$_2$Cl$_2$ were used in these experiments.

The femtosecond to nanosecond transient spectra of the excited states produced ~4 ps after the 387 nm flash irradiation of 10^{-4} M *fac*-(ferroceneCO$_2$)Re^I(CO)$_3$L complexes showed minor differences below 500 nm with the excited-state spectrum of *fac*-(Cl)Re^I(CO)$_3$L (L = phen, 2,2′-bpy) (Figure 4). However, they became nearly identical at all wavelengths after corrections were made for the differences in the ground-state spectra of the complexes. The spectra were therefore assigned to the ^{1}MLCT$_{Re\rightarrow L}$ excited state decaying in ~100 ps to long-lived triplet excited sates with lifetimes $t > 2$ ns. This assignment agrees with other literature reports.[33,34]

When *fac*-(ferroceneCO$_2$)Re^I(CO)$_3$(phen) and *fac*-(4-DMABCO$_2$) Re^I(CO)$_3$(phen) in CH$_3$CN were irradiated at 351 nm, the transient spectra observed after the 10 ns irradiation decayed biexponentially over a period of several microseconds. The oscillographic traces were fitted to two exponentials with lifetimes τ_{fast} and τ_{slow}. Transient spectra recorded with either complex at times $t \leq \tau_{fast}$, i.e., 20 ns after the flash, showed marked differences with the spectra of the ^{3}MLCT$_{Re\rightarrow L}$ excited states communicated in literature reports.[1,7,26,27] The transient spectra generated when these complexes were irradiated at 351

---

(33) Busby, M.; Gabrielsson, A.; Matosek, P.; Towrie, M.; Di Bilio, A. J.; Gray, H. B.; Vlček, A., Jr. *Inorg. Chem.* **2004**, *43*, 4994.

(34) Wolcan, E.; Feliz, M. R.; Alessandrini, J. L.; Ferraudi, G. *Inorg. Chem.* **2006**, *45*, 6666.

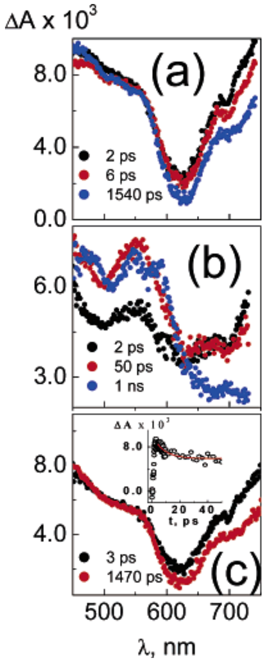

Figure 4. Comparison of the *t*-resolved absorption spectra recorded on a femtosecond to nanosecond time scale after the 387 nm flash irradiation of *fac*-(Cl)Re^{I}(CO)$_3$(phen) (a), *fac*-(4-DMABCO$_2$)Re^{I}-(CO)$_3$(phen) (b) and *fac*-(ferroceneCO$_2$)Re^{I}(CO)$_3$(phen) (c) solutions in CH$_3$CN. The concentrations of the complexes were $\sim 1 \times 10^{-4}$ M. Keys to the delays from the flash irradiation are given in the figure. A trace showing the formation and decay of the short-lived singlet excited states into the long-lived triplet excited states of *fac*-(ferroceneCO$_2$)Re^{I}(CO)$_3$(phen) is shown in the inset. The trace was obtained with the experimental conditions indicated above.

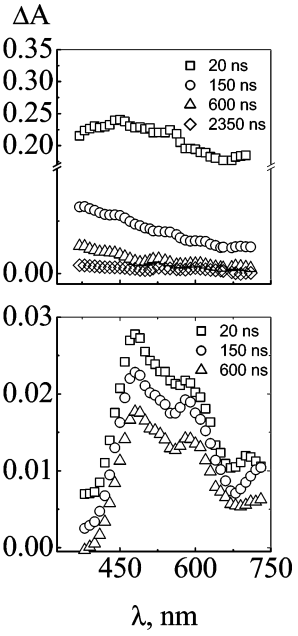

Figure 5. Transient spectra recorded on the nanosecond to microsecond time domain when 1×10^{-4} M *fac*-(ferroceneCO$_2$)-Re^{I}(CO)$_3$(phen) (top) and *fac*-(4-DMABCO$_2$)Re^{I}(CO)$_3$(phen) (bottom) in CH$_3$CN were flash-irradiated at 351 nm.

nm exhibited an intense maximum at ∼475 nm and a weak maximum at 580 nm (Figure 5).

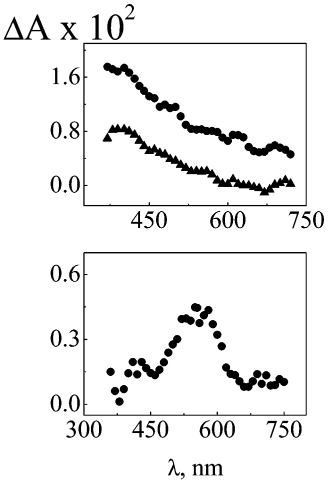

Figure 6. Transient spectra of the reduction products of *fac*-(ferroceneCO$_2$)Re^{I}(CO)$_3$(phen): (top) spectra generated when 1×10^{-4} M Re(I) complex and 0.1 M TEOA in CH$_3$CN were flash irradiated at 351 nm, recorded with 500 ns (●) and 700 ns (▲) delays from the flash irradiation; (bottom) spectrum recorded 11.5 ms after an N$_2$-saturated solution, $\sim 1 \times 10^{-4}$ M in Re(I) complex in CH$_3$OH, was pulse-radiolyzed.

In contrast to these observations, the 351 nm irradiation of *fac*-(ferroceneCO$_2$)Re^{I}(CO)$_3$(2,2′-bpy) in CH$_2$Cl$_2$ produced a spectrum with a maximum at 600 nm and another at a wavelength longer than 750 nm. Oscillographic traces for the decay of the transient absorbance in the 750 nm $> \lambda_{obs} \geq 600$ nm wavelength range were fitted to a biexponential with lifetimes $\tau_{fast} = 85$ ns and $\tau_{slow} = 400$ ns. The decay of the transient absorbance between 550 and 600 nm was fitted to a single exponential with a lifetime of $\tau = 180$ ns, nearly equal to the geometrical average, $(\tau_{fast}\tau_{slow})^{1/2} = 184$ ns. A lack of spectral resolution must be the reason for the monoexponential decay in the 550 nm $> \lambda_{obs} \geq 600$ nm wavelength range.

A good transient spectrum could not be photogenerated when *fac*-(ferroceneCO$_2$)Re^{I}(CO)$_3$(2,2′-bpy) was irradiated in CH$_3$CN, because of the small spectral changes produced with 351 nm laser flashes.

The transient spectrum departed, therefore, from the spectrum of ^{3}MLCT$_{Re\rightarrow phen}$, and only the weak feature at 550 nm could be related to a minor contribution, i.e., small concentration, from this excited state to the photogenerated transient spectra. On the basis of this convoluted contribution to the transient spectra, the presence of another excited state, coexisting with a small concentration of ^{3}MLCT$_{Re\rightarrow phen}$, must be intuited.

Self-Quenching and Photoreduction Products. The absorption spectrum of the ^{3}MLCT$_{Re\rightarrow phen}$ excited state, with maxima at λ_{max} 500 nm and λ_{max} >625 nm, was observed when 2×10^{-4} M *fac*-(ferroceneCO$_2$)Re^{I}(CO)$_3$(phen) in CH$_2$Cl$_2$ was flash-irradiated at 351 nm. This spectrum decayed monoexponentially with the lifetime $\tau = 170$ ns. Due to the concentration of *fac*-(ferroceneCO$_2$)Re^{I}(CO)$_3$(phen) used in the experiment, the self-quenching process makes this lifetime of the spectrum decay equal to the lifetime of the slow component of the luminescence. Therefore, the slow component in the decay of the transient spectrum and the luminescence must be assigned to the relaxation of the ^{3}MLCT$_{Re\rightarrow phen}$ excited states to the ground state.

2,2′.2″-Triethanolamine (TEOA) was used as an electron donor to the electronic excited states of *fac*-(RCO$_2$)Re^{I}(CO)$_3$-(phen) complexes. Flash irradiation of $\sim 8 \times 10^{-6}$ M *fac*-(RCO$_2$)Re^{I}(CO)$_3$(phen) in CH$_3$CN containing 0.1−1.0 M TEOA produced the spectra of the excited states on a 20−100 ns time scale and the spectra of reaction products at longer times (Figure 6). The spectra of these products exhibited an intense maximum at ∼450 nm and a weak maximum at ∼550 nm. The maximum at 550 nm was associated with the production of a small concentration of *fac*-(RCO$_2$)Re^{I}(CO)$_3$(phen^{-}) in a reaction

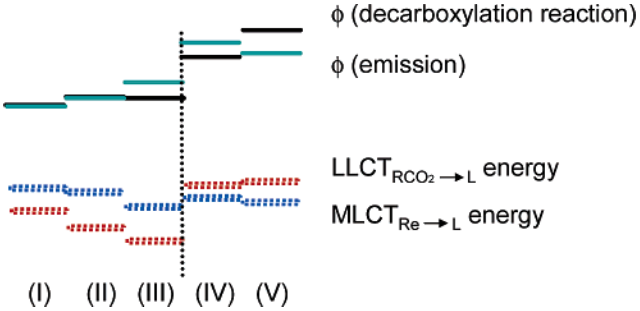

Figure 7. Relative ordering of the $LLCT_{RCO_2\to L}$ and $^3MLCT_{Re\to L}$ energies and values of the luminescence and photodecarboxylation quantum yields: (I) R = 4-DMAB, L = phen; (II) R = ferrocene, L = phen; (III) R = ferrocene, L = 2,2′-bpy; (IV) R = CH_3, L = phen; (V) R = CH_3, L = 2,2′-bpy. The vertical axis represents values relative to those of *fac*-(4-DMABCO$_2$)Re^I(CO)$_3$(phen) in arbitrary units. The dotted vertical line shows the point of inversion of the electronic levels and the associated change in photochemical properties.

between TEOA and the $^3MLCT_{Re\to phen}$ excited state. The product with the maximum at ~450 nm was attributed to a reaction between TEOA and another excited state. In accordance with the presence of two products decaying with different rates, the spectra of these products changed shape with probing time (Figure 6). The addition of the spectrum of the long-lived chromophore with the spectrum of pulse radiolytically generated *fac*-(RCO$_2$)Re^I(CO)$_3$(phen$^{\bullet-}$) accounts for the spectra of the products.

Pulse Radiolytically Generated Products. Pulse radiolytically generated e^-_{sol} reacted with 1×10^{-5} M *fac*-(RCO$_2$)Re^I(CO)$_3$L complexes in N_2-saturated methanolic solutions with rate constants $k \approx 10^{11}$ M^{-1} s^{-1}. The spectra of the reaction products were recorded 20 μs after the radiolytic pulse. They corresponded to Re(I) complexes, *fac*-(RCO$_2$)Re^I(CO)$_3$(L$^{\bullet-}$), with coordinated L$^{\bullet-}$ ligand radicals. The *fac*-(RCO$_2$)Re^I(CO)$_3$(L$^{\bullet-}$) products were stable for a time longer than 1 ms at the concentrations ($\leq 10^{-6}$ M) achieved in the radiolysis experiments (Figure 6).

In N_2O-saturated methanolic solutions of 1×10^{-5} M *fac*-(ferroceneCO$_2$)Re^I(CO)$_3$L or *fac*-(4-DMABCO$_2$)Re^I(CO)$_3$(phen), the reaction of $C^{\bullet}H_2OH$ radicals with these Re(I) complexes did not generate detectable concentrations of *fac*-(RCO$_2$)Re^I(CO)$_3$(L$^{\bullet-}$). The spectra of the reaction products agreed with the literature spectra of the oxidation products of the RCO_2^- ligands. Because of the standard potential of the $C^{\bullet}H_2OH$, H^+/CH_3OH couple, ~1.29 V vs NHE, $C^{\bullet}H_2OH$ radicals were able to oxidize the RCO_2^- ligands of the *fac*-(RCO$_2$)Re^I(CO)$_3$L complexes. The oxidation reactions were slow by comparison to the fast reactions occurring between $C^{\bullet}H_2OH$ radicals and only produced a very small concentration of the products.

Discussion

The photophysical and photochemical processes of *fac*-(RCO$_2$)Re^I(CO)$_3$L (R = ferrocene, 4-DMAB) are significantly different from the processes undergone by the reference complexes *fac*-(CH$_3$CO$_2$)Re^I(CO)$_3$L. Differences in the quantum yields of photodecarboxylation and in the kinetics of the charge-transfer excited-state relaxation must be associated with the higher energies of the RCO_2^- to L charge-transfer excited states in the reference complexes. On the basis of the redox potentials in Table 2, RCO_2^- to L charge-transfer excited states, $^3LLCT_{RCO_2\to L}$, are expected to have energies 4−49 kJ M^{-1} higher than those of the $^3MLCT_{Re\to L}$ excited states (Figure 7).

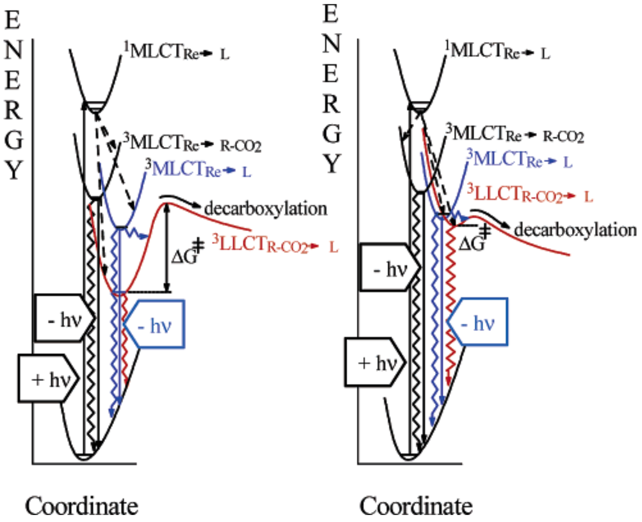

Figure 8. Idealized potential energy curves for the electronic levels of *fac*-(RCO$_2$)Re^I(CO)$_3$L (L = phen, 2,2′-bpy) complexes: (right) R = alkyl, aryl; (left) R = ferrocene, 4-DMAB. Dashed arrows indicate the conversion of the Franck−Condon singlet excited state to various nanosecond- to microsecond-lived triplet excited states on a time scale shorter than 5 ps. The activation energies, $\Delta G^‡$, for the photodecarboxylation process are relative to the 0 vibronic level of the photoreactive excited state (red curves).

The order of the excited states is inverted, however, in the *fac*-(RCO$_2$)Re^I(CO)$_3$L complexes, and the $^3LLCT_{RCO_2\to L}$ excited state is 77−54 kJ M^{-1} more stable than the $^3MLCT_{Re\to L}$ excited state (Figure 7). Changes in the photophysical and photochemical properties of the complexes follow this inversion in the order of the excited states (Figure 7). The abrupt change in the yields of the emission and photodecarboxylation is appreciable at the point of this level inversion. In contrast to the quantum yields of the photodecarboxylation, the ordering of the levels has a different effect on the lifetimes of the luminescence (Table 3), and it must be associated with an excited state different from $^3LLCT_{RCO_2\to L}$ and $^3MLCT_{Re\to L}$. This excited state was identified as one having chemical properties and spectroscopic features consistent with a transfer of charge from the Re to the RCO_2^- ligand (eq 7).

$$[^1A]fac\text{-}(RCO_2)Re^I(CO)_3L \underset{-\text{heat},\ -h\nu'}{\overset{h\nu}{\rightleftharpoons}} [^{1\text{ or }3}MLCT_{Re\to RCO_2}](RCO_2^{\bullet-})Re^{II}(CO)_3L \quad (7)$$

The optically induced transfer of charge from the Re(I) to the RCO_2^- ligand is justified on energetic terms. Because the electrochemical reduction of the carboxylate group in carboxylic acids and carboxylate complexes occurs at finite potentials (Table 2), optically induced metal-to-ligand charge-transfer transitions must be also possible processes from a thermochemical standpoint. On the basis of the redox potentials in Table 2, the energy of the 0−0 electronic transition to the $MLCT_{Re\to RCO_2}$ excited state (eq 7) occurs at energies smaller than the photonic energy of the light used for the irradiation of the complexes: i.e., 349 ± 2 nm. The $^3MLCT_{Re\to RCO_2}$ excited states, expected to be placed at lower energies than $^1MLCT_{Re\to RCO_2}$, can be populated from this spectroscopic excited state prior to or simultaneously with the $^3MLCT_{Re\to L}$ excited states (Figure 8). Indeed, the time-resolved absorption and emission spectra in Figures 3−5 can only be interpreted on the basis of two luminescent triplet excited states: i.e., the $^3MLCT_{Re\to L}$ and

^{3}MLCT$_{\mathrm{Re}\rightarrow\mathrm{RCO_2}}$ excited states. In contrast to the spectra of ^{3}MLCT$_{\mathrm{Re}\rightarrow\mathrm{L}}$ and the products of its reduction with TEA or TEOA, the absorption spectra of neither the ^{3}MLCT$_{\mathrm{Re}\rightarrow\mathrm{RCO_2}}$ excited state nor its reduction products will show features of the phen$^{\bullet-}$ or 2,2′-bpy$^{\bullet-}$ radical anions coordinated to either Re(I) or Re(II). The absence of L$^{\bullet-}$ spectral features was evident when the flash photolysis experiments were carried out with solutions of the *fac*-(ferroceneCO$_2$)Re$^{\mathrm{I}}$(CO)$_3$L complexes (Figures 5 and 6). Moreover, the lifetimes of the transients in Figure 5 are much longer than the lifetimes of the luminescence (Table 3). They could be assigned to a ^{3}MLCT$_{\mathrm{Re}\rightarrow\mathrm{RCO_2}}$ excited state that is much more weakly luminescent or is not luminescent at all.

Electron-transfer reactions where a carboxylate group is used as a bridge between an electron donor and an acceptor have shown that the carboxylate is a better electronic insulator than other bridging groups: e.g., halides and pseudohalides. Because of the insulating properties of the carboxylate, the radiationless relaxation of ^{3}MLCT$_{\mathrm{Re}\rightarrow\mathrm{RCO_2}}$ to the ground state, i.e., a process where a back transfer of charge from RCO$_2^{\bullet 2-}$ to the Re(II) takes place, can be slower than the radiationless relaxation of ^{3}MLCT$_{\mathrm{Re}\rightarrow\mathrm{L}}$ excited states. The localization of charge in R will also affect the rate of back electron transfer occurring in the radiationless relaxation, an effect that appears to be reflected in the lifetimes of the excited state.

On the basis of the ordering of the ^{3}MLCT$_{\mathrm{Re}\rightarrow\mathrm{L}}$ and ^{3}LLCT$_{\mathrm{RCO_2}\rightarrow\mathrm{L}}$ excited states (Figure 7), the self-quenching of the luminescence can be assigned to fast energy transfer reactions between complexes in the ^{3}MLCT$_{\mathrm{Re}\rightarrow\mathrm{L}}$ excited state and complexes in the ^{1}A ground state (eqs 8 and 9).

$$[^3\mathrm{MLCT}_{\mathrm{Re}\rightarrow\mathrm{L}}](\mathrm{RCO_2})\mathrm{Re^{II}(CO)_3(L^{\bullet-})} + [^1\mathrm{A}]\textit{fac}\text{-}(\mathrm{RCO_2})\mathrm{Re^{I}(CO)_3L} \rightarrow [^1\mathrm{A}]\textit{fac}\text{-}(\mathrm{RCO_2})\mathrm{Re^{I}(CO)_3L} + [^3\mathrm{LLCT}_{\mathrm{RCO_2}\rightarrow\mathrm{L}}](\mathrm{RCO_2^{\bullet+}})\mathrm{Re^{I}(CO)_3(L^{\bullet-})} \quad (8)$$

$$[^3\mathrm{LLCT}_{\mathrm{R-CO_2}\rightarrow\mathrm{L}}](\mathrm{RCO_2^{\bullet+}})\mathrm{Re^{I}(CO)_3(L^{\bullet-})} \xrightarrow{\text{fast}} [^1\mathrm{A}]\textit{fac}\text{-}(\mathrm{RCO_2})\mathrm{Re^{I}(CO)_3L} + \text{heat} \quad (9)$$

In spite of the change in the ordering of LLCT$_{\mathrm{RCO_2}\rightarrow\mathrm{L}}$ and MLCT$_{\mathrm{Re}\rightarrow\mathrm{L}}$ excited states in the *fac*-(RCO$_2$)Re$^{\mathrm{I}}$(CO)$_3$L complexes, the transient spectra observed ∼4 ps after the 387 nm irradiations must be assigned to ^{1}MLCT$_{\mathrm{Re}\rightarrow\mathrm{L}}$ excited states (Figure 4). This is possible because a small oscillator strength of the ^{1}LLCT$_{\mathrm{RCO_2}\rightarrow\mathrm{L}}$ ← ^{1}A electronic transition prevents ^{1}LLCT$_{\mathrm{RCO_2}\rightarrow\mathrm{L}}$ from being populated by the absorption of light. The conversion of the ^{1}MLCT$_{\mathrm{Re}\rightarrow\mathrm{L}}$ excited states into the excited states associated with the luminescence, i.e., ^{3}MLCT$_{\mathrm{Re}\rightarrow\mathrm{RCO_2}}$ and ^{3}MLCT$_{\mathrm{Re}\rightarrow\mathrm{L}}$, can be associated with a process observed on a femtosecond to 5 ps time scale (inset to Figure 4).

Because the spectroscopic features of the 2,2′-bpy$^{\bullet-}$ and phen$^{\bullet-}$ chromophores were very weak in the spectra of the long-lived *fac*-(ferroceneCO$_2$)Re$^{\mathrm{I}}$(CO)$_3$L excited states, the quantum yields of ^{3}LLCT$_{\mathrm{RCO_2}\rightarrow\mathrm{L}}$ and ^{3}MLCT$_{\mathrm{Re}\rightarrow\mathrm{L}}$ excited-state formation must be smaller than in the reference complexes. In the excited state spectrum of *fac*-(4-DMABCO$_2$)Re$^{\mathrm{I}}$(CO)$_3$(phen), the features of the phen$^{\bullet-}$ chromophore are more pronounced than in the *fac*-(ferroceneCO$_2$)Re$^{\mathrm{I}}$(CO)$_3$L complexes. While the ^{3}LLCT$_{\mathrm{RCO_2}\rightarrow\mathrm{L}}$ and ^{3}MLCT$_{\mathrm{Re}\rightarrow\mathrm{L}}$ excited states of *fac*-(4-DMABCO$_2$)Re$^{\mathrm{I}}$(CO)$_3$(phen) may be formed with yields larger than in the *fac*-(ferroceneCO$_2$)Re$^{\mathrm{I}}$(CO)$_3$L complexes, all of them have comparable quantum yields of photodecarboxylation (Table 1). The photodecarboxylation has been previously associated with ^{3}LLCT$_{\mathrm{RCO_2}\rightarrow\mathrm{L}}$ excited states. A smaller quantum yield of the ^{3}LLCT$_{\mathrm{RCO_2}\rightarrow\mathrm{L}}$ excited-state formation and a small efficiency of the excited-state reaction must be invoked to explain the diminished photoreactivity of the *fac*-(RCO$_2$)Re$^{\mathrm{I}}$(CO)$_3$L complexes in relationship to the reference complexes. The smaller efficiency of the photodecarboxylation in the ^{3}LLCT$_{\mathrm{RCO_2}\rightarrow\mathrm{L}}$ excited states implies a smaller rate constant of the decarboxylation reaction than in the reference complexes. A large stabilization of the LLCT excited states relative to the MLCT discussed in a previous paragraph can cause a significant increase in the activation energy of the decarboxylation reaction with a drop in the rate of this excited-state process (Figure 8).

Conclusions. The presence of ^{3}MLCT$_{\mathrm{Re}\rightarrow\mathrm{RCO_2}}$ excited states at accessible energies has a significant effect on the degradation of the Franck−Condon excited-state energy. It provides an unreactive channel, avoiding therein the photodecarboxylation of the carboxylate ligand. Groups R in the carboxylate ligand with the appropriate reduction potentials can be used to lower the energy of the ^{3}MLCT$_{\mathrm{Re}\rightarrow\mathrm{RCO_2}}$ excited states, where the photodecarboxylation is initiated, and inhibit the decomposition process.

Acknowledgment. G.F. and G.T.R. acknowledge support from the Office of Basic Energy Sciences of the U.S. Department of Energy. This is Contribution No. NDRL-4665 from the Notre Dame Radiation Laboratory. M.P.J. acknowledges support from the CICPBA and Fundación Antorchas. M.R.F. acknowledges support from the ANPCYT, Grant No. PICT 06-12610, and the CICPBA. E.W. acknowledges support from CONICET. R.O.L. acknowledges support from CONICET, Grant PIP N*o*. 0657/98.

Supporting Information Available: Figures giving the IR and NMR spectra and text giving assignments of the NMR spectra of the Re compounds. This material is available free of charge via the Internet at http://pubs.acs.org.

OM0604775